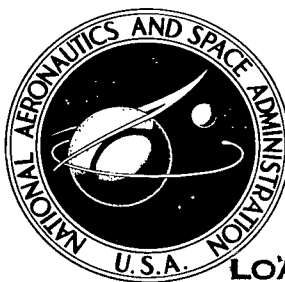


NASA TECHNICAL NOTE

NASA TN D-8339



NASA TN D-8339

p.1

LOAN COPY: R
AFWL TECHNICAL
KIRTLAND AFB

0134078



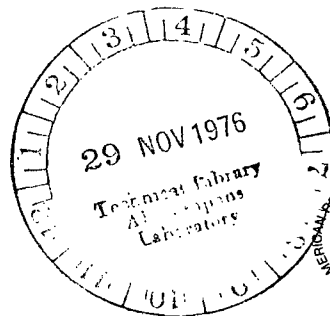
RY

RIM-SPOKE COMPOSITE FLYWHEELS - STRESS AND VIBRATION ANALYSIS

Christos C. Chamis and Louis J. Kiraly

Lewis Research Center

Cleveland, Ohio 44135





0134078

1. Report No. NASA TN D-8339		2. Government Accession No.		3. Recipient's Catalog No.	
4. Title and Subtitle RIM-SPOKE COMPOSITE FLYWHEELS - STRESS AND VIBRATION ANALYSIS				5. Report Date November 1976	
7. Author(s) Christos C. Chamis and Louis J. Kiraly				6. Performing Organization Code	
9. Performing Organization Name and Address Lewis Research Center National Aeronautics and Space Administration Cleveland, Ohio 44135				8. Performing Organization Report No. E-8657	
12. Sponsoring Agency Name and Address National Aeronautics and Space Administration Washington, D.C. 20546				10. Work Unit No. 506-17	
15. Supplementary Notes				11. Contract or Grant No.	
16. Abstract Elementary relations are used to determine the material utilization efficiency of a thin-wall rim composite flywheel over other configurations. An algorithm is generated for the automatic selection of the optimum composite material for a given thin-rim flywheel environment. Subsequently, the computer program NASTRAN is used to perform a detailed stress and vibration analysis of thin-wall cylindrical-shell rim-spoke single-rim and multirim composite flywheels for a specific application.				13. Type of Report and Period Covered Technical Note	
17. Key Words (Suggested by Author(s)) Composite materials; Fly wheels; Energy storage; Stress analysis; Mechanical engineering; Vibrational stress				14. Sponsoring Agency Code	
18. Distribution Statement Unclassified - unlimited STAR Category 39					
19. Security Classif. (of this report) Unclassified		20. Security Classif. (of this page) Unclassified		21. No. of Pages 21	22. Price* \$3.50

RIM-SPOKE COMPOSITE FLYWHEELS - STRESS AND VIBRATION ANALYSIS*

by Christos C. Chamis and Louis J. Kiraly

Lewis Research Center

SUMMARY

Elementary relations are used to determine the material utilization efficiency of a thin-wall rim composite flywheel compared with other configurations. An algorithm was generated for the automatic selection of the optimum composite material for a given thin-rim flywheel environment. Subsequently, the computer program NASTRAN was used to perform a detailed stress and vibration analysis of both single and multiple rim thin-wall cylindrical-shell rim-spoke composite flywheels for a specific application.

Preliminary results indicate that the flywheels investigated can be used to store power from a wind turbine generator and deliver it at the rate of 10 kilowatts for 4 days during which low winds prevent power generation from the turbine. The thin cylindrical rim is the most weight-efficient basic-element flywheel configuration for composites. Multirim flywheels combine both weight-efficient and volume efficient rims to optimize the total energy capacity of a single flywheel installation. NASTRAN can be used for the detail stress and structural dynamics analysis of both single and multirim flywheels.

INTRODUCTION

The use of fiber composite materials in flywheels offers several advantages over metal flywheels. The major advantages result primarily from the high longitudinal specific strength (strength/density) and high longitudinal specific stiffness (modulus/density) of composites compared with metals. Additional advantages offered by composites are (1) a large number of composites are available with a wide range of mechanical properties (fig. 1) from which selections can be made to meet diverse design requirements, (2) various flywheel configuration can be readily fabricated using the extensively developed filament winding capability that already exists, and (3) less material is required for containing flywheel bursts (reduced fragment kinetic energy).

Of the various composite flywheel configurations possible, the thin-wall cylindrical-

* A summary of this report was presented at the 1975 Flywheel Technology Symposium, Berkeley, Calif., Nov. 10-12, 1975.

shell rim-spoke configuration appears to utilize composites most efficiently. The distinct advantages of this configuration are

- (1) The rim is stressed primarily in the hoop direction in a centrifugal force field.
- (2) The rim can be fabricated using hoop windings only.
- (3) The thickness of the rim can be selected to minimize radial stresses resulting from the fabrication process (winding, thermal, and phase-change shrinkage) and the centrifugal forces.
- (4) The spokes can be sized to undergo radial deformation equivalent to that of the rim. For example, the spokes can be made from the same composite material, but with a pseudoisotropic laminate configuration. This will ideally yield a spoke modulus of one-third that of the hoop, which is the required condition for equivalent radial deformation. Equal radial spoke-rim deformation eliminates stress concentrations at the spoke-rim junction and the resulting induced bending in the rim (in lieu of designing a radially sliding joint between spoke and rim).
- (5) The concept is easily adaptable to multirim composite flywheels with specified clearance between rims.

Because the thin rims are in essence thin-wall cylindrical shells, they are readily susceptible to vibrate in one or more of their many natural frequencies within the wide range of flywheel operational rotation speeds (excitation frequencies). To assess the suitability of the composite thin-wall cylindrical-shell configuration in a flywheel environment, the vibration resistance of these configurations in the presence of a centrifugal force field needs to be determined. Therefore, an important objective of the present investigation was to perform detailed stress and vibration analyses of the thin-wall cylindrical-shell rim-spoke composite flywheel using NASTRAN to demonstrate

- (1) The adequacy of the thin-wall cylindrical-shell composite rim-spoke configuration for a specific flywheel application
- (2) The usage of available structural analysis tools to assess the potential vibration problem that might arise in such flywheels

Secondary objectives of the present investigation were (1) the demonstration of hoop-wound thin-rim superiority over other basic element flywheel configurations, (2) the selection of optimum composite material, and (3) the determination of the bounds on thin-rim wall thickness for negligible radial stresses.

SPECIFIC FLYWHEEL DESIGN EXAMPLE

The specific flywheel application investigation was for energy storage during calm or low wind conditions for a wind-turbine generator (such as shown in fig. 2) having the following assumed design requirements:

Required energy supply, days	4
Minimum reserve energy, percent	25
Charging rate, maximum, kW	100
Excess overspeed charging rate, percent	5
Power delivered by the flywheel during downtime, kW	10

The resulting total energy storage requirement is 5676 megajoules (1410 kW · h (4.5×10¹⁰ in-lb)).

APPROACH

The approach pursued in the present investigation is theoretical and consists of the following: derivation of material utilization index criteria, generation of an algorithm for the automatic selection of optimum composite materials, evaluation of radial stresses, use of NASTRAN to analyze a specific example. The details are described in the following sections.

Selection of the Most Efficient Basic-Element Composite Flywheel Configuration

The kinetic energy stored in the basic-element flywheel configurations depicted in figure 3 is readily determined using elementary strength of materials relations:

Flywheel configuration	Kinetic energy	Efficiency (normalized by $\frac{1}{2} W \omega^2 R^2$)
Thin-wall rim	$W\omega^2 R^2/2$	1.00
Rectangular bar	$W\omega^2 R^2/6$.33
Solid disk	$W\omega^2 R^2/4$.50

where R is the outer radius, ω is the rotational speed, and W is the total mass.

The results show that the thin-wall rim is the most efficient configuration for energy-stored per unit weight and a given $\omega^2 R^2$.

The maximum stress in the first two basic-element flywheel configurations (fig. 3) can also be determined using elementary strength of materials relations; in the third, the maximum stress is obtained from the elasticity solution of an orthotropic rotating

disk. The maximum hoop stresses are given by

Flywheel configuration	Maximum hoop stress
Thin-wall rim	$\rho\omega^2R^2$
Rectangular bar	$\rho\omega^2R^2/2$
Solid disk	$C\rho\omega^2R^2$

where $C = (N - \nu_{\theta r})/(3 + N)$, $N = (E_{\theta}/E_r)^{1/2}$, ρ is the material unit mass, $\nu_{\theta r}$ is the minor Poisson's ratio, E_{θ} the hoop (or longitudinal) modulus, and E_r the radial (or transverse) modulus. (The equation for the solid disk is from ref. 1.) For some of the composite materials given in table I, N and C have computed values as shown below.

Composite	Parameter	
	N	C
Isotropic material	1.00	0.18
Boron/aluminum	1.29	.24
Scotchply/epoxy	1.63	.30
Thornel 300/epoxy	3.00	.46
Boron/epoxy	3.33	.48
Kevlar 49/epoxy	4.66	.57
Modmor I/epoxy	5.48	.62

The value for Thornel 300/epoxy may produce singularity in the radial stress in a solid disk because this stress has the factor $1/(9 - N^2)$ (ref. 1).

As can be observed, the thin-wall rim generates the highest stress level for a given material and a given ω^2R^2 . It is noted that the solid disk made only with hoop windings is susceptible to transverse (radial) splitting. More will be said about radial splitting in a later section. Comparisons on a specific strength basis are shown in table II, where S_{L11T} denotes longitudinal tensile strength. As can be observed from the results in table II, the thin-wall rim has the highest rank without the risk of possible splitting due to radial stress.

It is noted that radial splitting may be prevented by suitable orientation of fibers, for example, pseudoisotropic layup in the plane of the disk. This layup configuration reduces the allowable stress by about a factor of four below that of the unidirectional configuration. The ranking of the solid disks in table II, therefore, must be multiplied

by four, which results in a rank of eight for a solid disk of Scotchply/epoxy relative to the thin-wall rim.

The important conclusion from the previous discussion is that the hoop-wound thin-wall rim is the most weight efficient basic-element flywheel configuration for composites.

Criteria for Sizing Spokes in Thin-Wall Rim-Spoke Composite Flywheels

Criteria for sizing spokes in thin-wall rim-spoke composite flywheel configurations may be derived by requiring that the radial deflection of the spoke equal the radial deflection of the rim. When this condition is satisfied, the following are also true: (1) the rim spoke system is statically determinate; (2) the stresses and deflections in the spokes and the rim are easily determined using elementary strength of materials relations; and (3) the spokes, fixed to the rim, do not induce bending in the rim because of differential radial expansion.

The resulting criterion for meeting the above condition in equation form is

$$\left(\frac{E_{rS}}{\rho_S}\right) = \frac{1}{3} \left(\frac{E_{\theta R}}{\rho_R}\right) \quad (1)$$

where E_{rS} is the spoke modulus in the radial direction, ρ_S is the spoke density, $E_{\theta R}$ is the rim modulus in the hoop direction, and ρ_R is the rim density. Therefore, a variety of choices are available to meet this criterion. A unique choice is to make the spoke from the same composite material as the rim but with a pseudoisotropic laminate configuration. The simplest pseudoisotropic laminate configurations are of the following type: $[0, \pm 60]_S$, $[0, 90 \pm 45]_S$, or even random orientation. The inplane modulus of the pseudoisotropic laminates is one-third of the longitudinal modulus. For example, the pseudoisotropic modulus of boron/epoxy (table I) is about 6.7×10^{10} pascals (9.7×10^{10} psi) and that of Kevlar-49/epoxy is 2.8×10^{10} pascals (4.1×10^6 psi).

The important conclusions from this discussion are that (1) criteria are easily derivable for sizing spokes and (2) a spoke made from the same composite as the rim but with pseudoisotropic layup satisfies the criterion for equal radial displacement in the rim and the spoke.

OPTIMAL MATERIAL SELECTION

Rim material selections were made using a computerized algorithm for multi-rimmed flywheel designs. Basically, the algorithm acts to choose each rim in such a

way as to maximize the total energy storage of the flywheel. This approach results in hoop stress levels approaching the strength capacity of the material in each rim.

A candidate materials list was used for material selection. The algorithm acts to select materials from this list on a rim by rim basis. The use of a candidate materials list allows definition of a wide range of possible materials. Furthermore, the use of such a list allows us to apply external constraints on material selection. For example, if environmental aspects or economic constraints were a factor, only those materials that satisfied these constraints would be included in the list. In this study the list contained several available high strength to weight ratio composites (table I), high strength steel alloys, and even lead. No further attempt was made to optimize the materials catalogued.

Calculation of the energy stored in a rotating rim leads to two expressions reflecting the energy storage efficiency of a given rim. The rotary inertia I , the radial displacement u , the hoop stress S_θ , and the energy stored in a rim T , are related by

$$I = 2\pi\rho htR^3 \left(1 + \frac{u}{R}\right)^2 \quad (2)$$

$$u = R \left(\frac{S_\theta}{E_\theta}\right) \quad (3)$$

$$S_\theta = \rho(R\omega)^2 \quad (4)$$

and

$$T = \frac{1}{2} I\omega^2 \quad (5)$$

where h , t , ρ , and R are, respectively, the rim height, thickness, mass density, and the midplane radius; and where ω represents the rotary speed. The energy storage is maximized when the hoop stress S_θ becomes equal to the fracture stress in the rim.

The volume and weight efficiency indices of a rim may now be expressed, respectively, as

$$\eta_V = \frac{T}{V} = S_\theta \left(\frac{t}{R}\right) \left(1 + \frac{S_\theta}{E_\theta}\right)^2 \quad (6)$$

and

$$\eta_w = \frac{T}{W} = \frac{1}{2} \left(\frac{S_\theta}{\rho} \right) \left(1 + \frac{S_\theta}{E_\theta} \right)^2 \quad (7)$$

These expressions lead us to the conclusions that

(1) The volume index of a rim is maximized with the highest strength material, regardless of weight.

(2) The weight index of a rim is maximized with the highest strength to weight ratio, regardless of the strength alone.

An installation efficiency index may now be defined for the practical implementation of a multirimmed flywheel. The installation index is a measure of the energy storage potential within a given flywheel containment. Rims reflecting both high volume indices and high weight indices are used for maximum installation efficiency index. For example, consider a high weight index rim operating at full capacity and designed to fit within some radius. The high weight index outer rim would be constructed using a material with a high strength-to-weight ratio (i. e. , a composite). Within the outer rim we may construct a high volume index rim using a stronger but denser material (i. e. , maraging steel). The energy storage capacity of the installation is thereby increased.

Multirimmed flywheel materials are selected to maximize the installation index by the computer algorithm. The computer program flow chart for this algorithm is depicted in figure 4. In addition to selecting the optimum rim material, the computer program acts as a preprocessor and generates the required NASTRAN input bulk data deck. We begin by defining the materials list, a maximum rim radius, a thickness to radius ratio, number of rims to be used, and the total energy to be stored. The highest strength-to-weight ratio material is selected for the outer rim, and the maximum rotational speed is calculated to fully load this material in hoop stress. The rim thickness, energy, and weight per unit height are calculated. If more rims need to be selected, the strength requirements at the next rim radius are determined and the most dense material satisfying the strength limitation is selected for the next rim. If the radial expansion of the current rim under loading is less than that of the previous (outer) rim, the condition is identified (so the NASTRAN preprocessor can generate a set of multiple point constraints between the rims). When all of the rims have been selected, the height of the flywheel as well as the resultant weight is calculated to meet the energy storage requirement. If the result is satisfactory, the required NASTRAN input bulk data deck is generated.

This algorithm was applied to a single rim and a 25-rim design. Specific cases of each type were examined using NASTRAN.

NASTRAN APPLICATION

The output of the material selection algorithm is used to generate the required NASTRAN input bulk data deck for all the rims. Each rim is modeled as a series of quadrilateral (CQUAD2) NASTRAN elements with centrifugal radial force loads applied (fig. 5). Rims that radially interfere at operational speed are identified and a set of multiple point constraints are applied at their boundaries. Selected rim materials are referenced and each of the rims are located in free space using NASTRAN single-point constraints instead of supporting spokes. Spokes of appropriate proportions were added later to study spoked flywheel cases (fig. 6).

The two designs selected for further study represent a single-rim design and a multi-rim design that appear to be of reasonable proportions for construction. Each design was studied in two configurations: (1) Rim flywheel with spokes and (2) rim flywheel without spokes. The four resulting configurations were then studied for stress and displacements in each of the following cases: (1) static analysis, (2) free vibration modal analysis, and (3) free vibration modal analysis with structural stiffening due to centrifugal and gravity loads.

Additional analysis was undertaken to determine stiffened mode vibrations for the flywheels at one-half of the rated speed. Limited studies of the effects of a concentrated mass and the change of vibration characteristics with changing rim thickness were also made.

Our goals with these cases were to

- (1) Determine the characteristics of thin rim-spoke composite superflywheels
 - (a) Modal characteristics
 - (b) Radial deformation
- (2) Identify the modal vibrations near the operating speeds of the flywheels
- (3) Establish the numerical procedures for the analysis and design of a multirim superflywheel installation

APPLICATION TO TWO SPECIFIC DESIGNS

Design Selection

The results of the computerized selection algorithm are plotted for families of single and multirim designs in figure 7. The single-rim and 25-rim flywheel designs are constrained by a rim thickness to radius ratio of 0.12, the unoptimized materials list, and a total energy storage requirement of 6120 megajoules (1410 kW · h (4.5×10^{10} in-lb)). Two designs selected for further study represented reasonable operating levels and proportions for construction. The selected designs are shown schematically in

figure 8. In this figure the basic properties and relative sizes of the single and multi-rim cases are identified.

The single-rim design is much lighter and much larger than the multirim design. The single rim represents a minimum weight condition, while the multirim design represents a maximum energy storage per containment size. Since the first five rims of the multirim design store 75 percent of the total energy, only these rims were included in the detailed NASTRAN analysis of stress and vibration.

Modal vibration frequencies for the two designs are summarized in table III. Modal vibrations are included for the rims alone and for the rims with spokes under both unloaded and centrifugally loaded conditions and at full and half speed operation. The central shaft of the flywheel assembly is considered to be infinitely rigid in all cases. In general, the resultant modal frequencies tended to reduce with the addition of spokes or with lower operating speeds. In the multirim case the frequencies listed correspond with a single rim (or rim-spoke assembly), which can vibrate independently of the rest of the structure. The addition of shaft compliance would have coupled this vibration to the rest of the flywheel structure.

The NASTRAN static stress analysis results for each rim are included in table IV, in which the stress levels and radial displacement of each rim at full operating speed are shown. In both design cases the flywheel is sized and operated to load the outermost rim to its strength capacity. When the amplitude of the lowest modal vibration is normalized to the steady-state radial deflection, the relative contributions of vibration stresses become the percentage values identified in the last column of table IV.

Dynamic Imbalance

The effects of a dynamic imbalance were briefly investigated for the single-rim design. The results are shown in table V. A 14.2-gram (1/2-oz) concentrated mass placed midway to the rim height increased the peak hoop stresses by 30 percent and increased the lowest modal vibration frequency 111 percent.

Perturbations of Design Parameters

A set of perturbations on the geometry design parameters were also run to briefly determine the effects of changing various aspects of the total design. The results (shown in table VI) indicate that modal frequencies may be controlled by changing sets of design parameters. In particular, we note that modal frequencies increase with increasing rim thickness, decreasing rim height, or increased rim-spoke interference. The results of the design perturbations are presented only as an indication of possible

parametric variations associated with this flywheel design, and may not be representative of rim-spoke flywheels in general.

VIBRATION MODE SHAPES

Modal Response

Modal responses are plotted in figures 9 to 13. These modal responses are generally represented as (1) rim bending modes, (2) bar bouncing modes, or (3) rim ringing modes. The rim ringing and bar bouncing modes are characterized by radially symmetric motions of the structure, and thus appear to cause minimal problems during operation. The bending modes, however, act to asymmetrically redistribute the rim mass with time. These modes are the most dangerous in the high rotary fields of an operational flywheel.

The bending mode vibrations do not occur in the operating ranges of the flywheels studied. However, more analysis for a finalized flywheel installation would be required. Detail design of a final flywheel structure requires that bending modes be identified and the flywheel be designed to decrease the probability of these modes in the operating range. Also, the possibility of subharmonic or superharmonic excitation should be carefully examined for these potentially destructive modes.

It appears that the rim bending modes can be most readily controlled by using more than two spokes at either end of a rim. This would decrease pivoting of the shell ends about the spoke.

SUMMARY OF RESULTS

The following major results were obtained from an investigation of the stress and vibration analyses of rim-spoke composite flywheels:

1. The hoop wound thin wall cylindrical rim is the most weight-efficient basic-element flywheel configuration for fiber composites.
2. Criteria are easily derivable for sizing spokes for rim-spoke flywheel. Spokes made from the same composite as the rim but with pseudoisotropic laminate configuration (ply layup) satisfy the criterion for each radial displacement in the rim and the spoke.
3. Multirim flywheels combine both weight efficient and volume efficient rims to optimize the total energy capacity of a single flywheel installation.
4. NASTRAN can be used for the detailed stress and vibration analysis of single-rim and multirim thin-wall cylindrical-shell rim-spoke composite flywheels. On a prelim-

inary design basis, the flywheel investigated can supply power during periods of low wind for 4 days at a power rate of 10 kilowatts.

5. Lewis developed multirim computer programs are effective in selecting optimal rim materials and in generating NASTRAN input bulk data decks for detailed analysis.

CONSIDERATIONS FOR FURTHER STUDY

The areas where further work is needed for the detailed design of multirim super flywheels are:

1. Selection of materials specifically chosen to optimize maximum rim strength to weight ratio and rim to rim compatibility
2. Investigation of filament winding techniques resulting in continuously variable strength and density rims (by variation of the filament to volume ratio). This technique would allow thicker rims with continuous mass density variation along the rim radius to optimize energy storage
3. Evaluation of subharmonic and superharmonic excitation of the potentially destructive rim bending vibration modes
4. Application of autobalancing devices/techniques to high speed flywheels.

Lewis Research Center,
National Aeronautics and Space Administration,
Cleveland, Ohio, June
506-17.

REFERENCE

1. Lekhnitskii, S. G.: Anisotropic Plates. Gordon and Beach, 1968.

TABLE I. - TYPICAL PROPERTIES OF UNIDIRECTIONAL FIBER COMPOSITES AT ROOM TEMPERATURE

Composite	Fiber volume ratio	Density	Thermal coefficient		Modulus			Poisson's ratio		Longitudinal strength		Transverse strength		Intra-laminar strength
			Longitudinal	Transverse	Longitudinal	Transverse	Shear	Major	Minor	Tensile	Compressive	Tensile	Compressive	
			----	g/cm ³	cm/cm/K		GPa			---	---	MPa		
Boron/epoxy AVCO5505	0.50	2.021	6.1	30.4	200	22	5.3	0.17	0.02	1364	1590	55.5	123.0	62.4
Boron/polyimide WRD9371	.49	1.993	4.9	28.4	220	14	7.6	.16	.02	1035	1083	11.0	62.4	25.7
Scotchply/epoxy 1009-26-5901	.72	2.132	3.8	16.7	60	25	12	.23	.09	1282	816	45.7	173.0	44.6
Modmor L/epoxy ERLA4617	.45	1.550	----	33.3	188	7.1	6.2	.10	----	836	877	41.6	195.0	61.0
Modmor I/polyimide WRD 9371	.45	1.550	0	25.4	215	4.9	4.5	.25	.02	802	648	14.7	69.9	21.6
Thornel 300/epoxy NARMCO 5208	.70	1.606	.02	22.5	180	10	6.9	.28	.01	1494	1693	40.1	245.0	67.2
Kevlar 49/epoxy CE-3305	.54	1.357	-2.90	56.3	84	4.8	2.8	.32	.02	1179	288	11.0	64.4	27.4
Boron/aluminum 6061-T6	.50	2.630	3.96	16.2	216	137	41	.23	.13	1480	1713	137.0	206.0	137.0
U.S. Customary units														
----	lb/in ³	in/in/°F		ksi			---	---	ksi					
Boron/epoxy AVCO5505	(a)	0.73	3.4×10 ⁻⁶	16.9×10 ⁻⁶	29.0×10 ³	3.15×10 ³	0.78×10 ³	(a)	(a)	199	232	8.10	17.90	9.10
Boron/polyimide WRD 9371	↓	.072	2.7	15.8	32.1	2.1	1.11	↓	↓	151	158	1.60	9.10	3.75
Scotchply/epoxy 1009-26-5901	↓	.077	2.1	9.3	8.8	3.6	1.74	↓	↓	187	119	6.67	25.30	6.50
Modmor I/epoxy ERLA4617	↓	.056	-----	18.5	27.5	1.03	.9	↓	↓	122	128	6.07	28.50	8.90
Modmor I/polyimide WRD 9371	↓	.056	0	14.1	31.3	.72	.65	↓	↓	117	94	2.15	10.20	3.15
Thornel 300/epoxy NARMCO 5208	↓	.058	.01	12.5	26.3	1.5	1.0	↓	↓	218	247	5.85	35.70	9.80
Kevlar 49/epoxy CE-3305	↓	.049	-1.60	31.3	12.2	.70	.41	↓	↓	172	42	1.60	9.40	4.00
Boron/aluminum 6061-T6	↓	.095	2.20	9.0	31.5	20.0	6.0	↓	↓	216	250	20.00	30.00	20.00

^aSame respective values for both SI and U.S. Customary Units.

TABLE II. - SPECIFIC STRENGTH COMPARISONS
OF BASIC-ELEMENT FLYWHEEL
CONFIGURATIONS

Flywheel configuration	Specific strength ^a	Rank
Thin-wall rim	1.00	1
Rectangular bar	.33	5
Solid disk: ^b		
Boron/aluminum	1.00	1
Scotchply/epoxy	.80	2
Boron/epoxy	.50	3
Kevlar 49/epoxy	.44	4

^aGiven in terms of longitudinal tensile composite strength, S_{L11T} .

^bPossible splitting due to radial stress.

TABLE III. - VIBRATION FREQUENCIES

[Single-rim rotation speed, 112.28 Hz; multirim rotation speed, 168.43 Hz.]

	Modes				
	1	2	3	4	5
	Frequency, Hz				
Single rim with supports:					
Normal modes	4.69	27.35	53.38	61.15	^a 113.4
Modes at 1/2 speed	31.26	55.58	61.02	^a 74.58	^a 127.6
Modes at full speed	36.38	-----	^a 179.45	^a 190.40	^a 208.4
Single rim without supports:					
Normal modes	^a 76.36	109.37	^a 111.15	^a 145.91	^a 158.88
Modes at full speed	91.64	298.6	^a 301.5	318.4	333.7
Multirim with supports:					
Normal modes	21.97	-----	157.24	^a 169.23	^a 178.50
Modes at 1/2 speed	24.42	-----	-----	-----	-----
Modes at full speed	25.11	149.76	164.57	165.69	175.52
Multirim without supports:					
Normal modes	92.54	-----	-----	-----	-----
Modes at full speed	149.62	-----	-----	-----	-----

^aTwo vibration mode shapes associated with this frequency.

TABLE IV. - HOOP STRESSES AND RIM DISPLACEMENTS

AT OPERATING SPEED

Flywheel design	Composite material	Radial displacement,		Rotational stress,		Lowest mode, maximum normalized stresses, percent
		mm	in.	mPa	ksi	
Single-rim (23 cm (9 in.) diam)	Thornel/epoxy	12.2	0.48	1500	218	0.1
Multirim (15 cm (6 in.) diam)	Thornel/epoxy	7.6	0.30	1500	218	0.1
	Thornel/epoxy	5.3	.21	1180	171	0
	Scotchply/epoxy	14.5	.57	1230	179	↓
	Boron/aluminum	3.6	.14	1200	174	
	Boron/aluminum	2.3	.09	930	136	

TABLE V. - EFFECTS OF DYNAMIC IMBALANCE

[One-half ounce concentrated mass placed at midpoint of rim height.]

	Value	Percent change
Maximum hoop stress, mPa (ksi)	195 (283)	30
Stiffened mode 1, Hz	86 (84)	111

TABLE VI. - DESIGN PERTURBATIONS

	Low modal frequency, Hz	Percent increase	High modal frequency, Hz	Percent increase
Normal single-rim at special spokes	12.09	--	198.42	---
31 Percent thickness increase ^a	-----	--	210.90	6
16 Percent rim height decrease	13.31	10	-----	---
Reduce modulus/density of spoke by 80 percent (e.g., make spoke steel)	17.95	40	-----	---

^aAs well as 31 percent increase in bar moment of inertia.

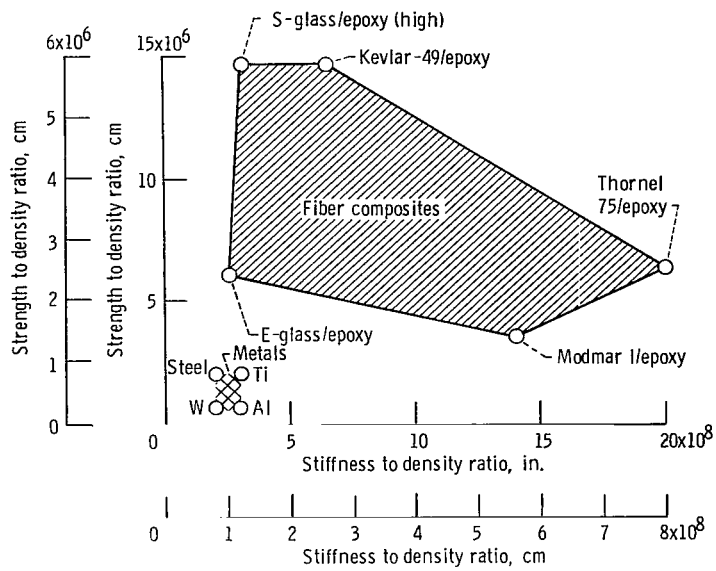


Figure 1. - Longitudinal composite strength and stiffness to density ratios of composites and metals.

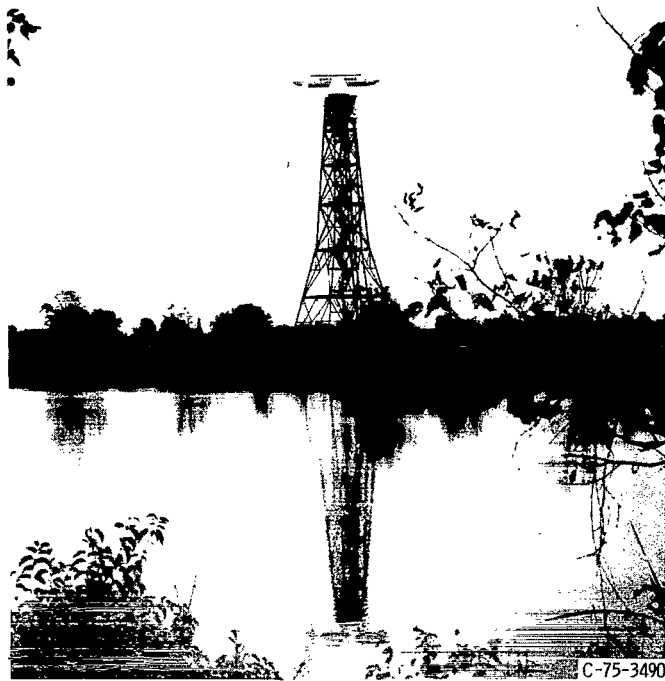


Figure 2. - ERDA-NASA 100-kilowatt wind turbine generator.

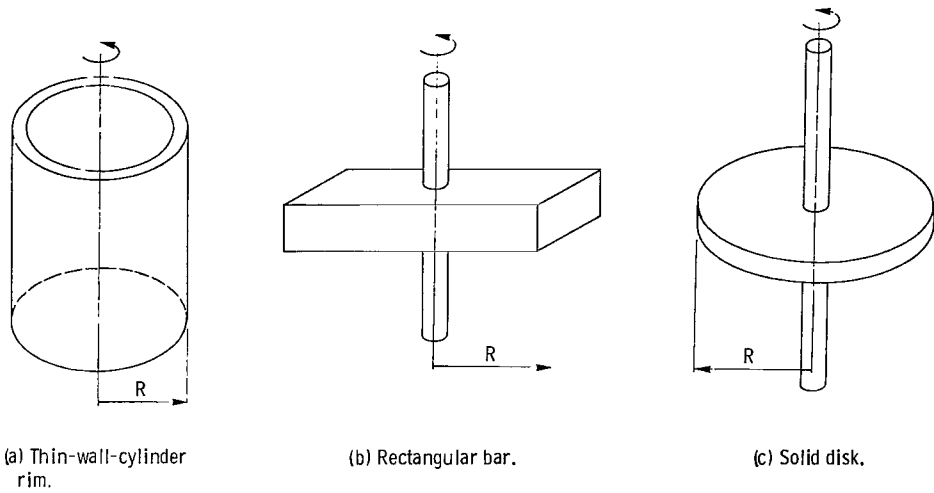


Figure 3. - Basic-element flywheel configurations.

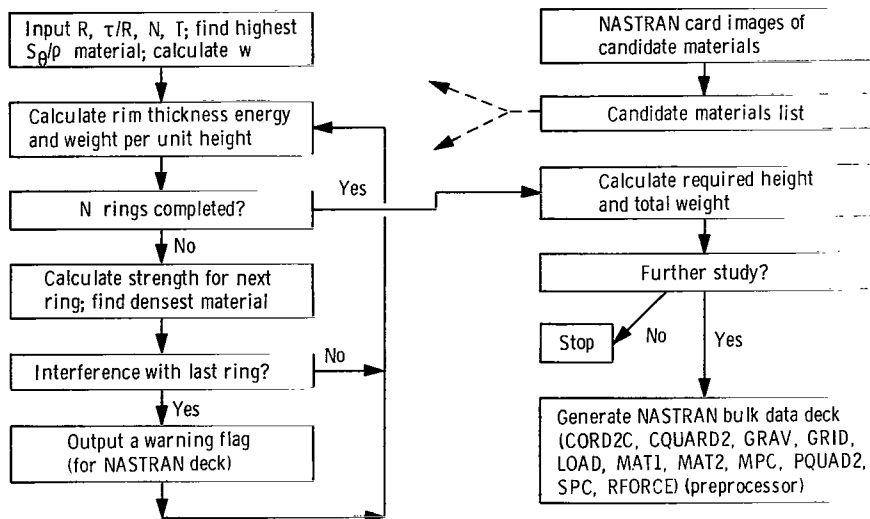


Figure 4. - Flow chart of algorithm for selecting rim materials.

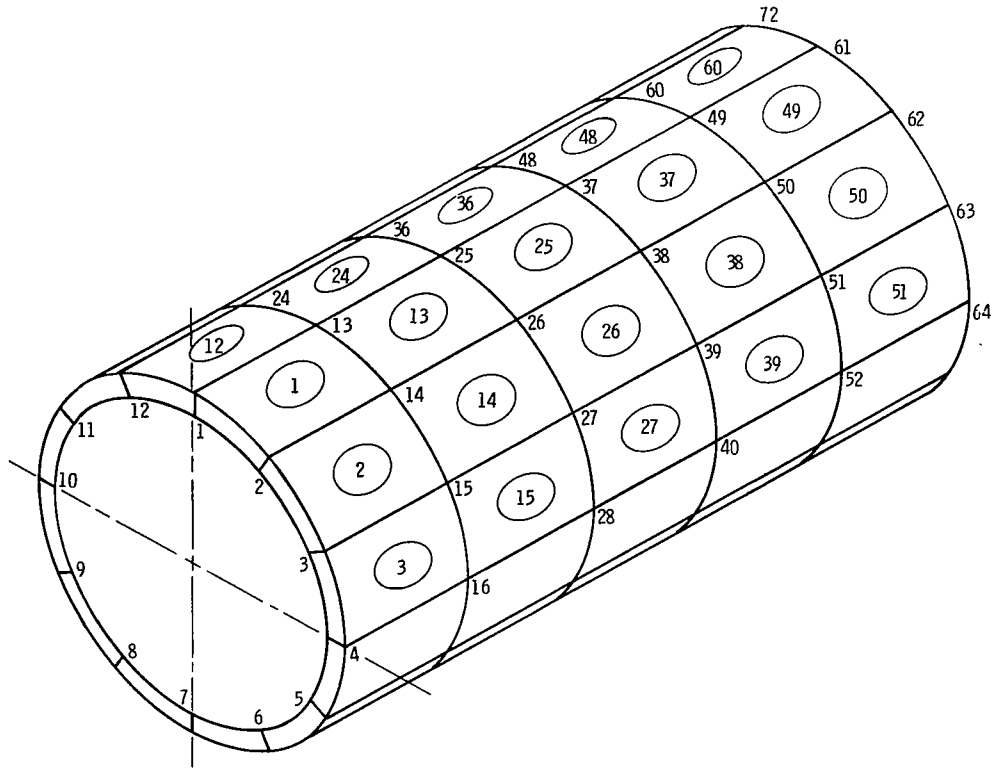
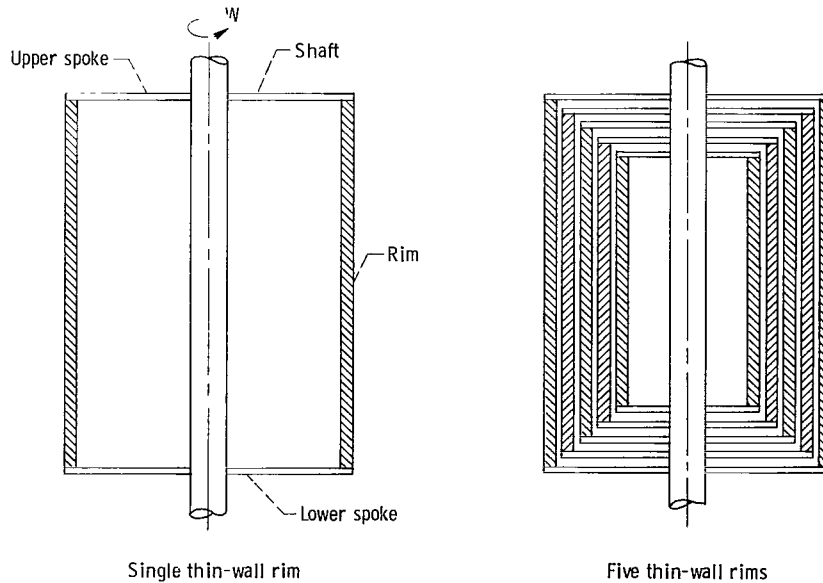


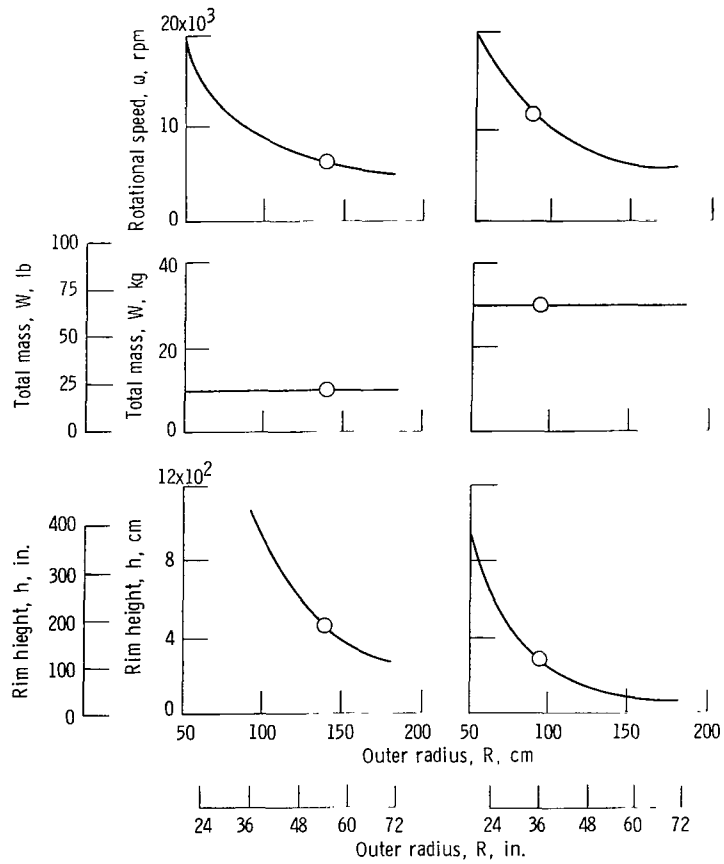
Figure 5. - Finite-element representation. Single-ring flywheel: 72 elements; 84 nodes. Multiring flywheels: 60 elements, 72 nodes per ring; and 300 elements, 360 nodes total.



Single thin-wall rim

Five thin-wall rims

Figure 6. - Schematics of flywheel configurations investigated.



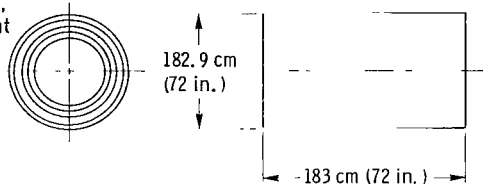
(a) Single rim. (b) 25 Rims.

Figure 7. - Algorithm results.



(a) Single rim. Material, Thornel/epoxy; rim diameter, 2.74 meters (9 ft); height, 4.72 meters (15 1/2 ft); total weight, 10 681 kilograms (23 548 lb); rotational speed, 6737 rpm.

Rim	Material	Outer radius cm (in.)	Rim thickness cm (in.)	Energy stored in rim, percent
1	Thornel/epoxy	91.44 (36.00)	10.97 (4.32)	27.5
2	Thornel/epoxy	81.08 (31.92)	9.73 (3.83)	17.0
3	Scotchply/epoxy	71.91 (28.31)	8.64 (3.40)	14.0
4	Boron/aluminum	63.78 (25.11)	7.65 (3.01)	10.5
5	Boron/aluminum	56.54 (22.26)	6.78 (2.67)	6.5
				75.5



(b) Multirim: 13 rings with steel core. Flywheel diameter, 1.83 meters (6 ft); height, 3 meters (10 ft); total weight, 29 360 kilograms (64 727 lb); rotational speed, 10 105 rpm. Outer five rings analyzed; weight of five rings, 11 761 kilograms (25 929 lb).

Figure 8. - Schematics of flywheel configurations analyzed.

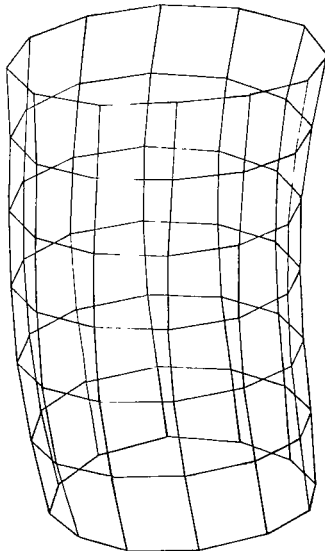


Figure 9. - Vibration mode shape of single rim composite flywheel. Rim bending mode at 99.9 hertz.

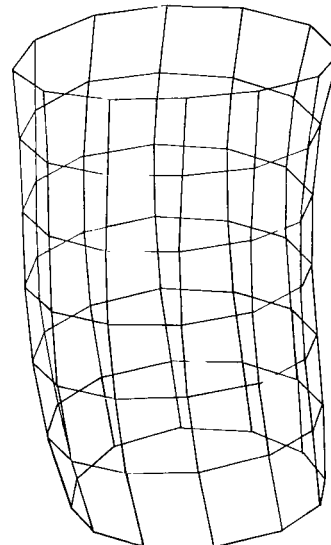
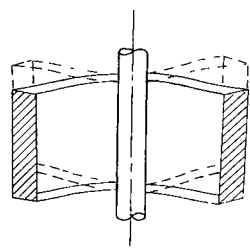
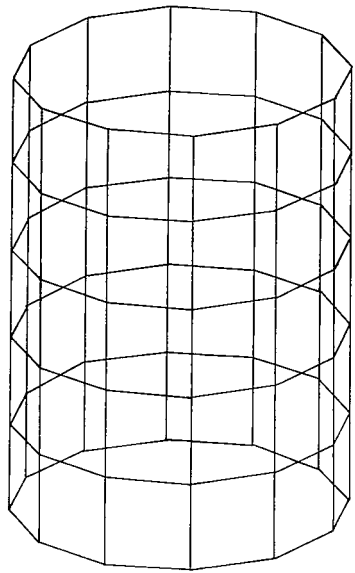
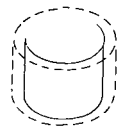
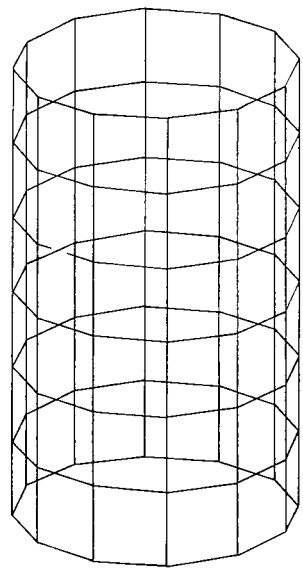


Figure 10. - Vibration mode shape of a single rim composite flywheel. Rim bending mode, 93.4 hertz.



Schematic illustrating spoke bouncing modes

Figure 11. - Vibration mode shape of a single rim composite flywheel. Spoke bouncing mode at 13.3 hertz.



Schematic illustrating rim ringing modes

Figure 12. - Vibration mode shape of a single rim composite flywheel. Rim ringing mode at 17.44 hertz.

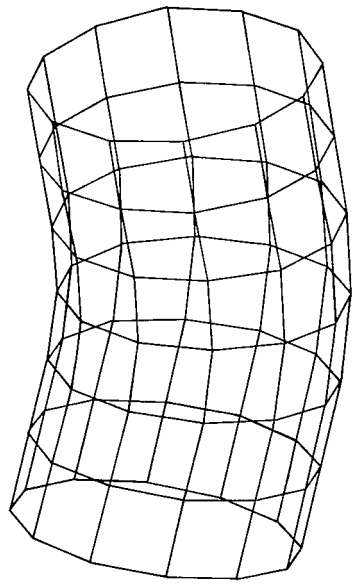


Figure 13. - Vibration mode shape of a single rim composite flywheel. Rim bending mode at 211 hertz.



875 001 C1 U D 761029 S00903DS
DEPT OF THE AIR FORCE
AF WEAPONS LABORATORY
ATTN: TECHNICAL LIBRARY (SUL)
KIRTLAND AFB NM 87117

POSTMASTER: If Undeliverable (Section 158
Postal Manual) Do Not Return

"The aeronautical and space activities of the United States shall be conducted so as to contribute . . . to the expansion of human knowledge of phenomena in the atmosphere and space. The Administration, shall provide for the widest practicable and appropriate dissemination of information concerning its activities and the results thereof."

NATIONAL AERONAUTICS AND SPACE ACT OF 1958

NASA SCIENTIFIC AND TECHNICAL PUBLICATIONS

TECHNICAL REPORTS: Scientific and technical information considered important, complete, and a lasting contribution to existing knowledge.

TECHNICAL NOTES: Information less broad in scope but nevertheless of importance as a contribution to existing knowledge.

TECHNICAL MEMORANDUMS: Information receiving limited distribution because of preliminary data, security classification, or other reasons. Also includes conference proceedings with either limited or unlimited distribution.

CONTRACTOR REPORTS: Scientific and technical information generated under a NASA contract or grant and considered an important contribution to existing knowledge.

TECHNICAL TRANSLATIONS: Information published in a foreign language considered to merit NASA distribution in English.

SPECIAL PUBLICATIONS: Information derived from or of value to NASA activities. Publications include final reports of major projects, monographs, data compilations, handbooks, sourcebooks, and special bibliographies.

TECHNOLOGY UTILIZATION PUBLICATIONS: Information on technology used by NASA that may be of particular interest in commercial and other non-aerospace applications. Publications include Tech Briefs, Technology Utilization Reports and Technology Surveys.

Details on the availability of these publications may be obtained from:

SCIENTIFIC AND TECHNICAL INFORMATION OFFICE

NATIONAL AERONAUTICS AND SPACE ADMINISTRATION

Washington, D.C. 20546